Exploring Inert Scalars at CLIC

Jan Kalinowski[a], Wojciech Kotlarski[b], Tania Robens[c], Dorota Sokolowska[a]
Aleksander Filip Żarnecki[a]

FACULTY OF PHYSICS
UNIVERSITY OF WARSAW

[a] Faculty of Physics, University of Warsaw
[b] Institut für Kern- und Teilchenphysik, TU Dresden
[c] MTA-DE Particle Physics Research Group, University of Debrecen

CLIC Detector and Physics Collaboration Meeting 2018
Physics and Analysis session
August 28, 2018

Outline

Results (and write-up) prepared for CLIC BSM report.

Inert Doublet Model

One of the simplest extensions of the Standard Model (SM).
The scalar sector consists of two doublets:

- Φ_S is the SM–like Higgs doublet,
- Φ_D (inert doublet) has four additional scalars H, A, $H^\pm$.

$$\Phi_S = \begin{pmatrix} G^\pm \\ \frac{v+h+iG^0}{\sqrt{2}} \end{pmatrix} \qquad \Phi_D = \begin{pmatrix} H^\pm \\ \frac{H+iA}{\sqrt{2}} \end{pmatrix}$$

Inert Doublet Model

One of the simplest extensions of the Standard Model (SM).
The scalar sector consists of two doublets:

- Φ_S is the SM–like Higgs doublet,
- Φ_D (inert doublet) has four additional scalars H, A, $H^\pm$.

$$\Phi_S = \begin{pmatrix} G^\pm \\ \frac{v+h+iG^0}{\sqrt{2}} \end{pmatrix} \qquad \Phi_D = \begin{pmatrix} H^\pm \\ \frac{H+iA}{\sqrt{2}} \end{pmatrix}$$

We assume a discrete Z_2 symmetry under which

- SM Higgs doublet Φ_S is *even*: $\Phi_S \rightarrow \Phi_S$ (also other SM→SM)
- inert doublet Φ_D is *odd*: $\Phi_D \rightarrow -\Phi_D$.

⇒ Yukawa-type interactions only for Higgs doublet (Φ_S).
The inert doublet (Φ_D) does not interact with the SM fermions!

⇒ The lightest inert particle is stable: a natural candidate for dark matter!
We assume the neutral scalar H is the dark matter particle.

$$m_H < m_A,\ m_{H^\pm}$$

Inert Doublet Model

After EWSB, the model contains a priori seven free parameters.

Two parameters can be fixed from the Standard Model (v, m_h).

We are left with five free parameters, which we take as:

$\Rightarrow$ three inert scalar masses: m_H, m_A, $m_{H^\pm}$

$\Rightarrow$ two couplings, eg. λ_2 and $\lambda_{345} = \lambda_3 + \lambda_4 + \lambda_5$

Inert Doublet Model

After EWSB, the model contains a priori seven free parameters.

Two parameters can be fixed from the Standard Model (v, m_h).

We are left with five free parameters, which we take as:

$\Rightarrow$ three inert scalar masses: m_H, m_A, $m_{H^\pm}$

$\Rightarrow$ two couplings, eg. λ_2 and $\lambda_{345} = \lambda_3 + \lambda_4 + \lambda_5$

Inert scalars couplings to γ, $W^\pm$ and Z determined by SM parameters

$\Rightarrow$ well established predictions for production and decay rates!

We scanned the IDM parameter space looking for scenarios consistent with current theoretical and experimental constraints, for masses up to 1 TeV.

For details and previous IDM parameter scan results see:

- Agnieszka Ilnicka, Maria Krawczyk, and Tania Robens, *Inert Doublet Model in light of LHC Run I and astrophysical data*, Phys. Rev. D93(5):055026, 2016, arXiv:1508.01671.
- Agnieszka Ilnicka, Tania Robens, and Tim Stefaniak, *Constraining Extended Scalar Sectors at the LHC and beyond*, Mod. Phys. Lett. A33(10n11):1830007, 2018, arXiv:1803.03594.

IDM benchmark points

Out of about 15'000 points consistent with all considered constraints, we chose 43 benchmark points (23 accessible at 380 GeV) for detailed studies:

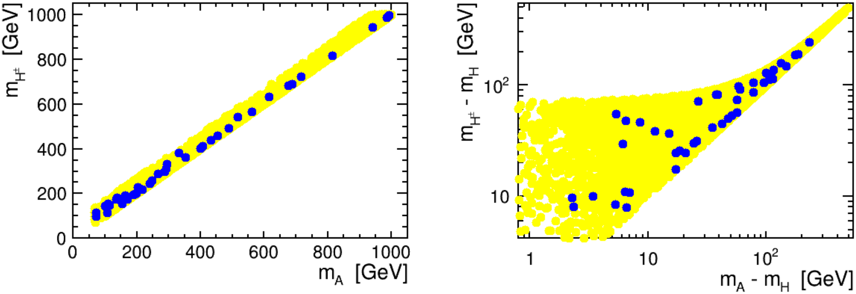

The selection was arbitrary, but we tried to

- cover wide range of scalar masses and the mass splittings
- get significant contribution to the relic density

For list of benchmark point parameters, see backup slides

Analysis strategy

Production of IDM scalars at CLIC dominated by two processes:

$$e^+e^- \to A\ \ H \qquad\qquad e^+e^- \to H^+H^-$$

Leading-order cross sections for inert scalar production processes at 380 GeV:

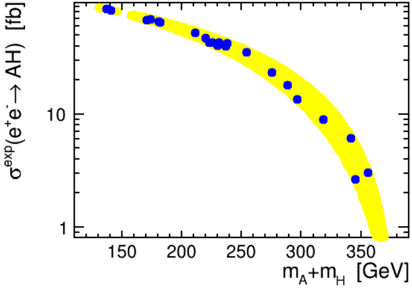

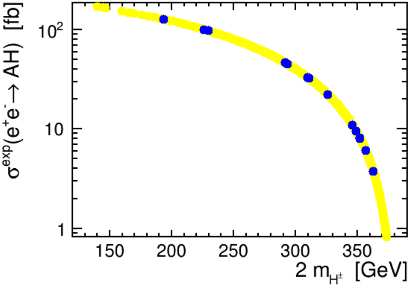

Beam luminosity spectra not taken into account

Analysis strategy

Production of IDM scalars at CLIC dominated by two processes:

$$e^+e^- \to A\ \ H \qquad\qquad e^+e^- \to H^+H^-$$

Leading-order cross sections for inert scalar production processes at 1.5 TeV:

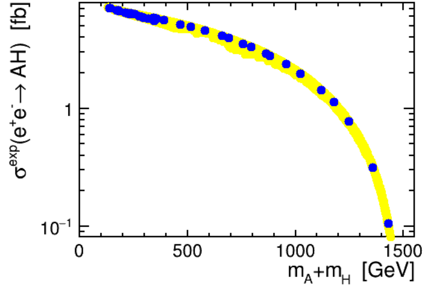

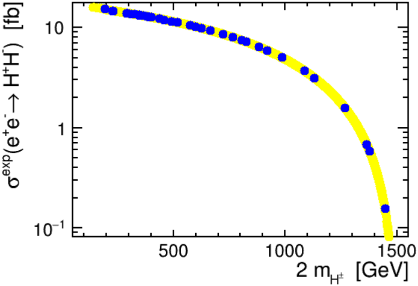

Beam luminosity spectra not taken into account

Analysis strategy

Lepton pair production can be a signature of the AH production process followed by the A decay:

$$e^+e^- \rightarrow HA \rightarrow HHZ^{(\star)} \rightarrow HH\mu^+\mu^-$$

while the production of the different flavour lepton pair is the expected signature for H^+H^- production:

$$e^+e^- \rightarrow H^+H^- \rightarrow HHW^{+(*)}W^{-(*)} \rightarrow HH\ell^+\ell'^-\nu\bar{\nu}'$$

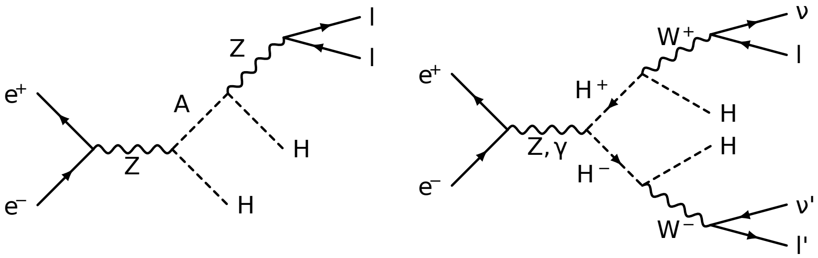

Analysis strategy

We consider two possible final state signatures:

- moun pair production, $\mu^+\mu^-$, for AH production
- electron-muon pair production, $\mu^+ e^-$ or $e^+\mu^-$, for H^+H^- production

Both channels include contributions from AH and H^+H^- production!
In particular due to leptonic tau decays.

Signal and background samples were generator with WHizard 2.2.8
based on the dedicated IDM model implementation in SARAH,
parameter files for benchmark scenarios were prepared using SPheno 4.0.3

CLIC luminosity spectra taken into account (1.4 TeV scaled to 1.5 TeV)

Generator level cuts reflecting detector acceptance:

- require lepton energy $E_l > 5\,\text{GeV}$ and lepton angle $\Theta_l > 100\,\text{mrad}$
- no ISR photon with $E_\gamma > 10\,\text{GeV}$ and $\Theta_\gamma > 100\,\text{mrad}$

Muon pair invariant mass, $M_{\mu\mu}$, as a function of the lepton pair longitudinal momentum, $P_Z^{\mu\mu}$, for BP1 scenario and SM background, at 380 GeV

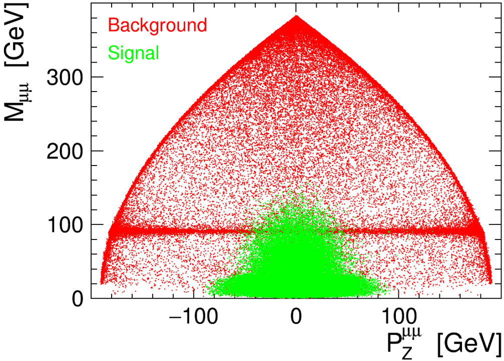

Background dominated by muon pair production $(e^+e^- \rightarrow \mu^+\mu^-)$ at nominal energy and radiative events $(e^+e^- \rightarrow \mu^+\mu^-\gamma)$
⇒ apply pre-selection cuts: $M_{\mu\mu} < 100\,\mathrm{GeV}$ and $|P_Z^{\mu\mu}| < 140\,\mathrm{GeV}$

Distributions of the kinematic variables describing the leptonic final state

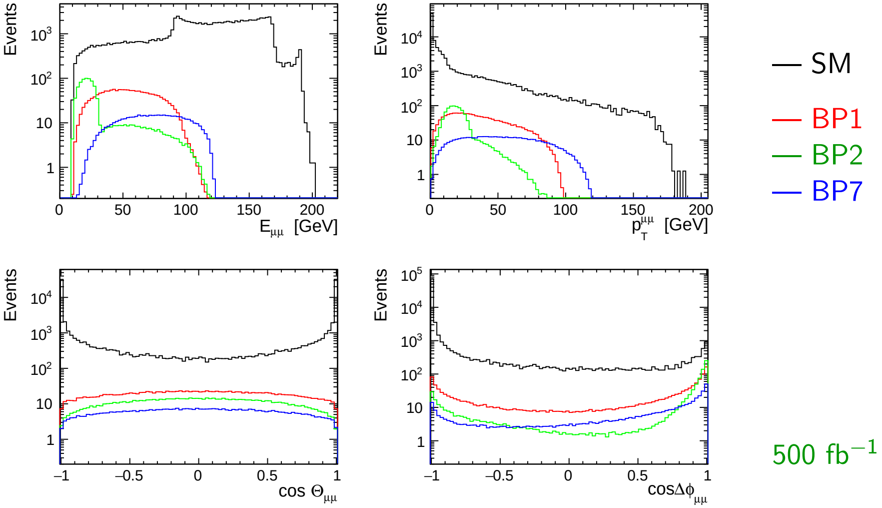

Cut based approach

Lepton pair invariant mass distribution after selection cuts 500 fb^{-1}

- pair energy
  $E_{\mu\mu} < 100\,\text{GeV}$
- transverse momentum
  $p_T^{\mu\mu} > 10\,\text{GeV}$
- production angle
  $30^\circ < \Theta_{\mu\mu} < 150^\circ$
- azimuthal distance
  $|\Delta\varphi_{\mu\mu}| < \frac{\pi}{2}$

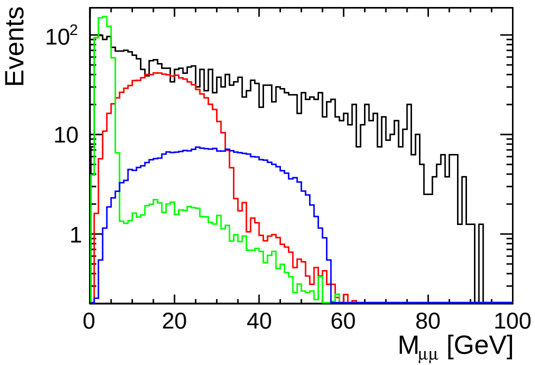

Considered IDM scenarios result in the visible event excess
15σ, 11σ and 5σ, for BP1, BP2 and BP7

Multivariate analysis

BDT classifier with 8 input variables used for selection of signal events

Response distribution for $\mu\mu$ channel: BP1 scenario and SM background
500 fb^{-1} at $\sqrt{s} = 380$ GeV

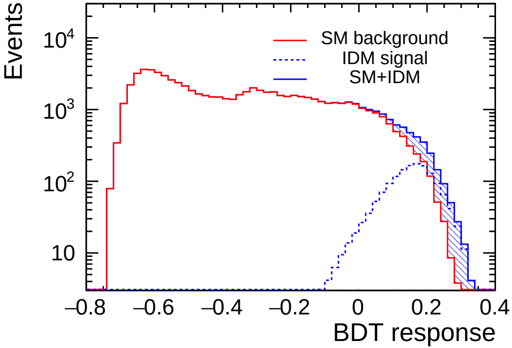

$\Rightarrow$ signal significance of about 19.5σ for BDT> 0.11

Multivariate analysis

Summary of results for the considered benchmark scenarios

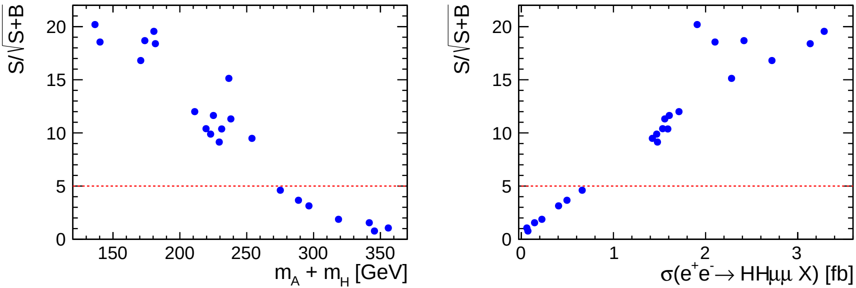

Expected significance mainly related to the *AH* production cross section

$5\,\sigma$ observation possible for signal cross section above about 1 fb (in the $\mu^+\mu^-$ channel)

$\Rightarrow$ neutral inert scalar mass sum below about 260 GeV

Charged scalar production @ 380 GeV

Distributions of the kinematic variables describing the leptonic final state

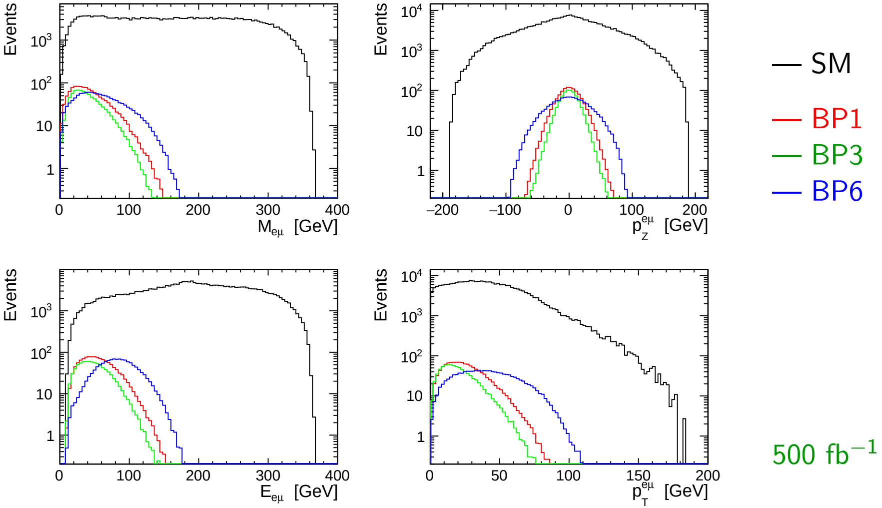

Multivariate analysis

BDT classifier response distribution for $e\mu$ channel:
BP1 scenario and SM background $500\ \mathrm{fb}^{-1}$ at $\sqrt{s} = 380$ GeV

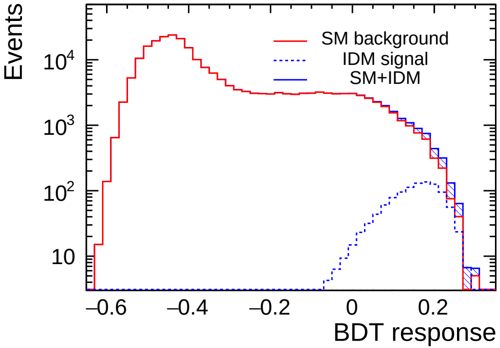

$\Rightarrow$ signal significance of about 12σ for BDT> 0.13

Charged scalar production @ 380 GeV

Multivariate analysis

Summary of results for the considered benchmark scenarios

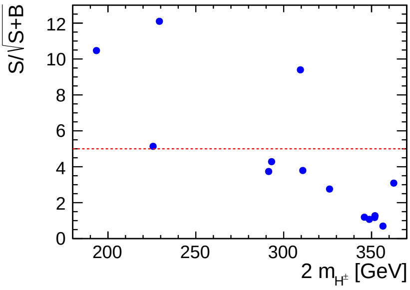

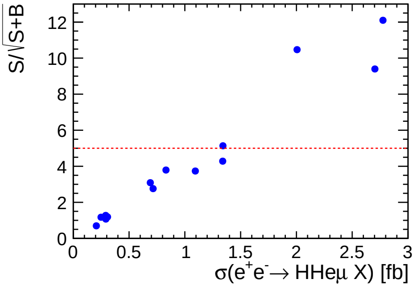

Expected significance mainly related to the H^+H^- production cross section

$5\,\sigma$ observation possible for signal cross section above about 1.5 fb

$\Rightarrow$ charged scalar masses up to about 140 GeV

significant differences are visible between different benchmark scenarios, mainly depending on the mass difference between charged and neutral inert scalar

Prospects for high energy running

Same analysis procedure applied for high energy CLIC running:

$1500\,\text{fb}^{-1}$ at 1.5 TeV and $3000\,\text{fb}^{-1}$ at 3 TeV

AH signature ($\mu^+\mu^-$)

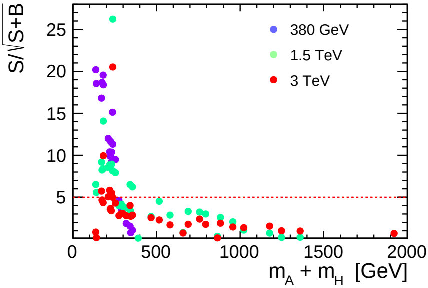

H^+H^- signature ($\mu^\pm e^\mp$)

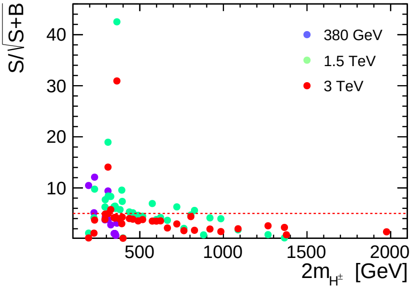

Moderate increase in discovery reach for 1.5 TeV:

- neutral scalar production: $m_A + m_H < 450$ GeV (260 GeV @ 380 GeV)
- charged scalar production: $m_{H^\pm} < 450$ GeV (140 GeV @ 380 GeV)

Prospects for high energy running

As for 380 GeV, significance of the observation mainly driven by the signal production cross section (in $\mu\mu$ or $e\mu$ channel) + integrated luminosity

Significance scaled to the same integrated luminosity of $500\,\text{fb}^{-1}$

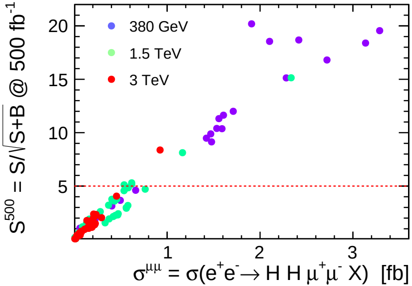

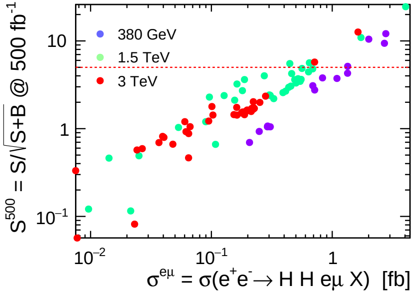

Slope of the significance vs cross section dependence can be used as a measure of the experimental sensitivity

Ratio of the expected significance (scaled to $500\,\mathrm{fb}^{-1}$) to the signal cross section in the considered channel, as a function of the scalar mass splitting

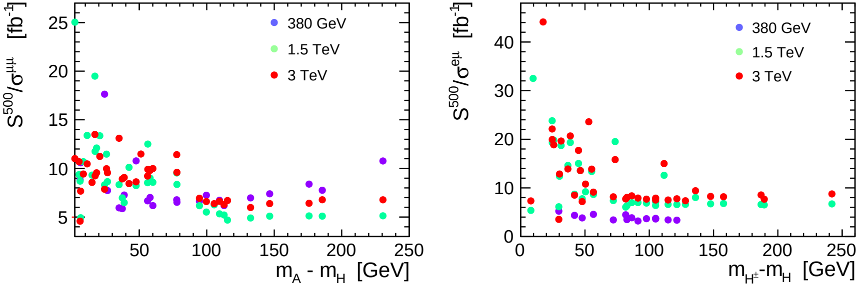

For both channels: sensitivity tends to be better at low mass splittings

when virtual Z or W boson produced in decay chain

For AH search: sensitivity decreases with energy for large mass splittings

For H^+H^-: sensitivity increases with energy for all mass differences

Conclusions

Prospects for discovery of inert scalars studied for three CLIC stages, running at 380 GeV, 1.5 TeV and 3 TeV

Conclusions

Prospects for discovery of inert scalars studied for three CLIC stages, running at 380 GeV, 1.5 TeV and 3 TeV

Low mass scenarios can be observed with high significance in the di-muon channel already at the first stage of CLIC, up to $m_A + m_H \sim 260\,\text{GeV}$

$m_{H^\pm} \sim 140\,\text{GeV}$ for $e\mu$ channel

Conclusions

Prospects for discovery of inert scalars studied for three CLIC stages, running at 380 GeV, 1.5 TeV and 3 TeV

Low mass scenarios can be observed with high significance in the di-muon channel already at the first stage of CLIC, up to $m_A + m_H \sim 260$ GeV

$m_{H^\pm} \sim 140$ GeV for $e\mu$ channel

The discovery reach is extended to $\sim$450 GeV when running at 1.5 TeV

Conclusions

Prospects for discovery of inert scalars studied for three CLIC stages, running at 380 GeV, 1.5 TeV and 3 TeV

Low mass scenarios can be observed with high significance in the di-muon channel already at the first stage of CLIC, up to $m_A + m_H \sim 260\,\text{GeV}$

$m_{H^\pm} \sim 140\,\text{GeV}$ for $e\mu$ channel

The discovery reach is extended to $\sim$450 GeV when running at 1.5 TeV

No improvement with 3 TeV running (cross sections too low)

Conclusions

Prospects for discovery of inert scalars studied for three CLIC stages, running at 380 GeV, 1.5 TeV and 3 TeV

Low mass scenarios can be observed with high significance in the di-muon channel already at the first stage of CLIC, up to $m_A + m_H \sim 260\,\text{GeV}$
$m_{H^\pm} \sim 140\,\text{GeV}$ for $e\mu$ channel

The discovery reach is extended to $\sim$450 GeV when running at 1.5 TeV

No improvement with 3 TeV running (cross sections too low)

Much higher significance can be expected for H^+H^- production in the semi-leptonic final state (isolated lepton and two jets or one massive jet)

- energy and invariant mass recontruction for one of W bosons
  $\Rightarrow$ better signal-background separation
- much larger branching fraction compared to $e\mu$: 2.25% $\Rightarrow$ 28.6%
  $\Rightarrow$ significance increase by at least a factor of 3
  $\Rightarrow$ estimated discovery reach up to $m_{H^\pm} \sim 700\,\text{GeV}$

Plans

In addition to the CLIC BSM report contribution we plan to prepare

- e-print/paper with detailed description for benchmark selection
- e-print/paper with more details on IDM phenomenology at e^+e^- colliders, covering also 250 and 500 GeV

Plans

In addition to the CLIC BSM report contribution we plan to prepare

- e-print/paper with detailed description for benchmark selection
- e-print/paper with more details on IDM phenomenology at e^+e^- colliders, covering also 250 and 500 GeV

Full simulation study of selected benchmark point(s) will follow, in particular for semi-leptonic channel (looks promissing)

Should we consider 380 GeV? Or go directly to 1.5 TeV?

Thank you!

Additional references

Inert Doublet Model

- Nilendra G. Deshpande and Ernest Ma, *Pattern of Symmetry Breaking with Two Higgs Doublets*, Phys. Rev. D18:2574, 1978.
- Laura Lopez Honorez and Carlos E. Yaguna, *The inert doublet model of dark matter revisited*, JHEP 09:046, 2010, 1003.3125.
- Ethan Dolle, Xinyu Miao, Shufang Su, and Brooks Thomas, *Dilepton Signals in the Inert Doublet Model*, Phys. Rev. D81:035003, 2010, 0909.3094.
- A. Goudelis, B. Herrmann, and O. Stål, *Dark matter in the Inert Doublet Model after the discovery of a Higgs-like boson at the LHC*, JHEP 09:106, 2013, 1303.3010.

Software

- Wolfgang Kilian, Thorsten Ohl, and Jurgen Reuter, *WHIZARD: Simulating Multi-Particle Processes at LHC and ILC*, Eur. Phys. J. C71:1742, 2011, arXiv:0708.4233.
- Florian Staub, *Exploring new models in all detail with SARAH*, Adv. High Energy Phys. 2015:840780, 2015, arXiv:1503.04200.
- Werner Porod, *SPheno, a program for calculating supersymmetric spectra, SUSY particle decays and SUSY particle production at e+ e- colliders*, Comput. Phys. Commun. 153:275–315, 2003, hep-ph/0301101.
- Andreas Hoecker, Peter Speckmayer, Joerg Stelzer, Jan Therhaag, Eckhard von Toerne, and Helge Voss, *TMVA: Toolkit for Multivariate Data Analysis*, PoS ACAT:040, 2007, physics/0703039.

IDM benchmark points

Constraints on inert scalar masses and couplings

- Theoretical
  - vacuum stability at tree level
  - perturbative unitarity
  - global minimum of the potential
- Experimental
  - (SM-like) Higgs boson mass and signal strenghts from LHC
  - Total widths of W and Z boson
  - Agreement with electroweak precision observables
  - Exclusion from SUSY searches at LEP and LHC experiments.
  - Lower limit on $H^{\pm}$ width from long-lived charged particle searches
  - Direct bound by the dark matter nucleon scattering (LUX, XENON1T)
  - Planck limit on relic density

Low mass IDM benchmark points

No.	M_H	M_A	$M_{H\pm}$	λ_2	λ_{345}	$\Omega_c h^2$
BP1	72.77	107.8	114.6	1.445	-0.004407	0.1201
BP2	65	71.53	112.8	0.7791	0.0004	0.07081
BP3	67.07	73.22	96.73	0	0.00738	0.06162
BP4	73.68	100.1	145.7	2.086	-0.004407	0.08925
BP5	55.34	115.4	146.6	0.01257	0.0052	0.1196
BP6	72.14	109.5	154.8	0.01257	-0.00234	0.1171
BP7	76.55	134.6	174.4	1.948	0.0044	0.0314
BP8	70.91	148.7	175.9	0.4398	0.0051	0.124
BP9	56.78	166.2	178.2	0.5027	0.00338	0.08127
BP10	76.69	154.6	163	3.921	0.0096	0.02814
BP11	98.88	155	155.4	1.181	-0.0628	0.002737
BP12	58.31	171.1	173	0.5404	0.00762	0.00641
BP13	99.65	138.5	181.3	2.463	0.0532	0.001255
BP14	71.03	165.6	176	0.3393	0.00596	0.1184
BP15	71.03	217.7	218.7	0.7665	0.00214	0.1222
BP16	71.33	203.8	229.1	1.03	-0.00122	0.1221
BP17	55.46	241.1	244.9	0.289	-0.00484	0.1202
BP18	147	194.6	197.4	0.387	-0.018	0.001772
BP19	165.8	190.1	196	2.768	-0.004	0.002841
BP20	191.8	198.4	199.7	1.508	0.008	0.008494
BP21	57.48	288	299.5	0.9299	0.00192	0.1195
BP22	71.42	247.2	258.4	1.043	-0.00406	0.1243
BP23	62.69	162.4	190.8	2.639	0.0056	0.06404

High mass IDM benchmark points

No.	M_H	M_A	$M_{H\pm}$	λ_2	λ_{345}	$\Omega_c h^2$
HP1	176	291.4	312	1.49	-0.1035	0.0007216
HP2	557	562.3	565.4	4.045	-0.1385	0.07209
HP3	560	616.3	633.5	3.38	-0.0895	0.001129
HP4	571	676.5	682.5	1.98	-0.471	0.0005635
HP5	671	688.1	688.4	1.377	-0.1455	0.02447
HP6	713	716.4	723	2.88	0.2885	0.03515
HP7	807	813.4	818	3.667	0.299	0.03239
HP8	933	940	943.8	2.974	-0.2435	0.09639
HP9	935	986.2	988	2.484	-0.5795	0.002796
HP10	990	992.4	998.1	3.334	-0.051	0.1248
HP11	250.5	265.5	287.2	3.908	-0.1501	0.00535
HP12	286.1	294.6	332.5	3.292	0.1121	0.00277
HP13	336	353.3	360.6	2.488	-0.1064	0.00937
HP14	326.6	331.9	381.8	0.02513	-0.06267	0.00356
HP15	357.6	400	402.6	2.061	-0.2375	0.00346
HP16	387.8	406.1	413.5	0.8168	-0.2083	0.0116
HP17	430.9	433.2	440.6	3.003	0.08299	0.0327
HP18	428.2	454	459.7	3.87	-0.2812	0.00858
HP19	467.9	488.6	492.3	4.122	-0.252	0.0139
HP20	505.2	516.6	543.8	2.538	-0.354	0.00887

Signal processes for $\mu^+\mu^-$ final state

$$
\begin{aligned}
e^+e^- &\rightarrow \mu^+\mu^- \, HH, \\
&\rightarrow \mu^+\mu^-\nu_\mu\bar{\nu}_\mu \, HH, \\
&\rightarrow \tau^+\mu^-\nu_\tau\bar{\nu}_\mu \, HH, \;\; \mu^+\tau^-\nu_\mu\bar{\nu}_\tau \, HH, \\
&\rightarrow \tau^+\tau^- \, HH, \;\; \tau^+\tau^-\nu_\tau\bar{\nu}_\tau \, HH. \\
&\quad \text{with} \tau^\pm \rightarrow \mu^\pm\nu\nu
\end{aligned}
$$

Signal processes for $e^\pm\mu^\mp$ final state

$$
\begin{aligned}
e^+e^- &\rightarrow \mu^+\nu_\mu \, e^-\bar{\nu}_e \, HH, \;\; e^+\nu_e \, \mu^-\bar{\nu}_\mu \, HH, \\
&\rightarrow \mu^+\nu_\mu \, \tau^-\bar{\nu}_\tau \, HH, \;\; \tau^+\nu_\tau \, \mu^-\bar{\nu}_\mu \, HH, \\
&\rightarrow e^+\nu_e \, \tau^-\bar{\nu}_\tau \, HH, \;\; \tau^+\nu_\tau \, e^-\bar{\nu}_e \, HH, \\
&\rightarrow \tau^+ \, \tau^- \, HH, \;\; \tau^+\nu_\tau \, \tau^-\bar{\nu}_\tau \, HH,
\end{aligned}
$$

BDT input variables

Input variables describing the kinematics of the dilepton final state:

- total energy of the muon pair, E_{ll};
- dilepton invariant mass, M_{ll};
- dilepton transverse momentum, p_T^{ll};
- polar angle of the dilepton pair, Θ_{ll} ;
- Lorentz boost of the dilepton pair, $\beta_{ll} = p_{ll}/E_{ll}$;
- ℓ^- production angle with respect to the beam direction, calculated in the dilepton center-of-mass frame, $\Theta_l^\star$
- ℓ^- production angle with respect to the dilepton pair momentum direction, calculated in the dilepton center-of-mass frame, $\angle^\star(\ell, \ell\ell)$,
- reconstructed missing (recoil) mass M_{miss} (calculated assuming nominal e^+e^- collision energy),